

INCREASED MECHANICAL PROPERTIES THROUGH THE ADDITION OF ZR TO GRCOP-84

David L. Ellis and Bradley A. Lerch
NASA Glenn Research Center
Cleveland, OH 44135

ABSTRACT

GRCop-84 (Cu-8 at.% Cr-4 at.% Nb) has shown exceptional mechanical properties above 932 °F (773 K). However, its properties below 932 °F (773 K) are inferior to precipitation strengthened alloys such as Cu-Cr, Cu-Zr and Cu-Cr-Zr when they are in the fully aged, hard-drawn condition. It has been noted that the addition of small amounts of Zr, typically 0.1 wt.% to 0.5 wt.%, can greatly enhance the mechanical properties of copper-based alloys. Limited testing was conducted upon GRCop-84 with an addition of 0.4 wt.% Zr to determine its tensile, creep and low cycle fatigue (LCF) properties. Very large increases in strength (up to 68%) and ductility (up to 123%) were observed at both room temperature and 932 °F (773 K). Creep properties at 932 °F (773 K) demonstrated more than an order of magnitude decrease in the creep rate relative to unmodified GRCop-84 with a corresponding order of magnitude increase in creep life. Limited LCF testing showed that the modified alloy had a comparable LCF life at room temperature, but it was capable of sustaining a much higher load. While more testing and composition optimization are required, the addition of Zr to GRCop-84 has shown clear benefits to mechanical properties.

INTRODUCTION

GRCop-84 (Cu-8 at.% Cr-4 at.% Nb) was developed by NASA for regeneratively cooled reusable launch vehicle main engine combustion chamber liners, which require good high temperature properties. It also has potential for other high temperature, high conductivity applications. However, it suffers from lower mechanical properties than competitive precipitation strengthened alloys such as Cu-Zr, Cu-Cr and Cu-Cr-Zr below 932 °F (773 K) and especially below 572 °F (573 K)¹. Options were examined for improving the low temperature mechanical properties while maintaining high thermal conductivity. Comparing similar Cu-based alloys with and without Zr¹⁻⁵, the addition of small amounts of Zr, typically 0.1 wt.% to 0.5 wt.%, greatly increased the properties of similar alloys, e.g., Cu versus Cu-0.15 wt.% Zr⁵. It was hypothesized that the addition of similar amounts of Zr to GRCop-84 would result in improved mechanical properties below 932 °F (773 K). An experimental alloy, designated GRCop-84Z, was produced and limited testing was conducted to survey its mechanical properties.

When Zr is added to Cu, it forms an intermetallic compound Cu_xZr . The value of x has been reported as 4, 4.5 and 5 by various sources⁶. Zr can also form Cr-Zr compounds, but prior work with Cu-Cr-Zr alloys has shown that the Cr-Zr compounds are not stable in the ternary alloys⁷. The Cu_xZr compounds can be dissolved in solid Cu at high temperatures using a solutioning heat treatment and later precipitated as fine particles to give significant strengthening. Prior work with Cu-Zr and Cu-Cr-Zr also indicates that Zr can help retain cold work at elevated temperatures¹. That was not examined in this work due to time limitations, but, based upon prior work with Cu-Zr^{1,8}, the tensile strength and creep strength of GRCop-84Z would benefit from cold work.

EXPERIMENTAL PROCEDURE

POWDER PRODUCTION AND CONSOLIDATION

GRCop-84 is a powder metallurgy Cu-based alloy. GRCop-84Z used the same techniques and production methods. The GRCop-84Z powder was atomized at Crucible Research (now ATI Powder

Metals) in Pittsburgh, PA. The powder was sieved to -140 mesh (<106 μm diameter). The powder was placed into a 6-inch (15.2 cm) diameter 1018 carbon steel can, and the can was evacuated. The powder was consolidated by direct hot extrusion at HC Starck in Coldwater, MI to make a 1.5-inch x 2.5-inch (3.8 cm x 6.4 cm) rectangular bar. Samples from the powder and the consolidated bar were taken for chemistry.

HEAT TREATMENT DEVELOPMENT

A two step heat treatment was developed for GRCo-84 Zr. The work was largely based upon the heat treatments of the Cu-0.15 wt.% Zr and other precipitation strengthened copper alloys⁹. Samples were solution heat treated at 1652 °F, 1697 °F and 1742 °F (1173 K, 1198 K and 1223 K) for 30 minutes followed by a water quench. A combination of hardness change and microstructural examinations were used to determine the best solution heat treatment.

Once the solutioning temperature was established, aging was conducted at 797 °F, 887 °F and 977 °F (698 K, 748 K and 798 K). Based upon the prior work with Cu-Zr and Cu-Cr-Zr alloys, the lower temperature is likely suitable for a cold worked sample while the higher temperature is likely suitable for an annealed sample. The aging time was varied from 30 to 90 minutes.

MECHANICAL TESTING

Following solution heat treatment and aging, tensile, creep and LCF samples were machined from the bars. The tensile and creep test specimens were identical and conformed to ASTM Standard E 8¹⁰. The design used 3/8-inch 18 tpi threaded ends and a reduced gauge section that was 0.240-inch (5.8 mm) in diameter. The overall length of the sample was 3.2-inches (80 mm). The LCF specimens used a sample with 0.400-inch (10.3 mm) diameter smooth ends and a reduced section 0.250-inch (6.4 mm) in diameter. The overall length was 6-inches (152 mm).

Tensile testing was conducted at room temperature and 932 °F (773 K). Strain rate control was used during the test, and the strain rate selected was 0.005 min^{-1} . An extensometer was used to measure the strain up to 15%. To determine the strain above 15%, the crosshead displacement was used. It was assumed that the displacement was equal to the elongation of the samples' reduced sections since the samples' ultimate tensile strength (UTS) had been achieved by then, and the samples were necking. For the elevated temperature tests, the samples were heated at ≥ 1800 °F/h (≥ 1000 K/h), the temperature stabilized, and the test conducted. Flowing Ar was used to minimize oxidation.

Creep testing was conducted in vacuum at 932 °F (773 K) at 15.8, 18.2 and 20.9 ksi (109.2, 125.5 and 144.5 MPa). After evacuating the chamber, the samples were heated at ≥ 1800 °F/h (≥ 1000 K/h) under a 1 lb (0.5 kg) load to maintain the load train aligned during heating. Once at temperature, the temperature was stabilized, the load removed and the full load applied using dead weights. Displacement was measured using a continuously variable resistor attached to the load train outside of the vacuum chamber. A data acquisition system periodically recorded the displacement during the test.

LCF testing was conducted using a hydraulic MTS load frame. The specimens were tested in strain control with the strain being measured by an extensometer. Total strain ranges ($\Delta\epsilon_{Total}$) of 0.7%, 0.8%, 1.0% and 1.2% were used in the testing, and the strain rate was 0.002 sec^{-1} in all tests. The testing used a fully reversed ($R = -1$) triangular waveform for the strain with no dwell. All testing was conducted at room temperature.

MICROSCOPY

Optical microscopy was used to examine the alloy in the as-extruded and heat treated conditions. Samples were mounted in Bakelite or epoxy and mechanically polished through 0.05 μm colloidal silica. The material was etched using a solution of 25% NH_4OH – 50% $(\text{NH}_4)_2\text{S}_2\text{O}_8$ solution (2.5 g/100 ml solution) – 25% H_2O that was diluted by adding five parts distilled water to one part etchant. Dilution was required to prevent over-etching of the samples. Optical microscopy was also used to examine the fracture surfaces after testing.

The samples were first examined optically to determine the grain structure and to determine if any new phases were evident. The samples were then examined in a scanning electron microscope (SEM) with an energy dispersive spectrometer (EDS) system for elemental X-ray mapping to identify the distribution of the elements, in particular Zr.

X-RAY DIFFRACTION

X-ray diffraction was used to determine the phases present in the as-extruded GRCop-84Z specimen. Since this had the slowest cooling rate of any sample, it was assumed that the phases would attain their maximum volume fraction and size in this sample. A Cu X-ray tube and K- α radiation were used to identify the major phases present. Multiple slow scans were conducted to determine which phases were present. Angles that corresponded to possible Cu-Zr phases received additional scans.

RESULTS

CHEMICAL COMPOSITION

The results for the powder provided by ATI Powder Metals and the results for the as-extruded bar determined at NASA GRC are given in Table 1. The target composition is also given. A small amount of Hf and Fe were detected. The Hf is an impurity in the Zr melt stock, and Fe is an impurity in the Cr melt stock. Neither should have an effect upon the results at the levels observed¹¹. The Zr level is slightly higher than specified but well within the range where benefits are expected.

Table 1 – GRCop-84Z Chemical Composition

Element	Cr	Nb	Fe	Hf	O	Zr	Cu
Target							
Weight Percent	6.65	5.85	<0.005	<0.002	<0.040	0.35	Bal.
Atomic Percent	8.17	4.02				0.25	Bal.
Crucible Research Powder							
Weight Percent	6.75	5.86	0.004	0.005	0.0205	0.44	Bal.
Atomic Percent	8.29	4.03				0.31	Bal.
NASA GRC Extruded Bar							
Weight Percent	6.61	5.86	<0.005	<0.001	0.0103	0.43	Bal.
Atomic Percent	8.12	4.03				0.30	Bal.

PHASE IDENTIFICATION

The X-ray diffraction results from the as-extruded GRCop-84Z are shown in Figure 1. The major phases were Cu which is the matrix for the alloy and Cr_2Nb , the strengthening phase for GRCop-84 which makes up about 14% of the alloy by volume. The four minor phases identified were Cr, CuZr_2 , Cu_5Zr and $\text{Nb}_{0.6}\text{Cr}_{0.4}\text{O}_2$. Elemental Cr is present because there is a slight excess of Cr in the alloy to lower the

activity of Nb in the Cr₂Nb and to prevent possible hydrogen embrittlement. The Nb_{0.6}Cr_{0.4}O₂ most likely was a tenacious surface oxide. CuZr₂ was not expected since it is the most Zr-rich of the several Cu-Zr compounds³. It may be indicative of Zr not being well dissolved and mixed into the melt prior to atomization. Most likely, subsequent solution heat treatments would dissolve the CuZr₂ into the Cu and reduce or eliminate this phase. Cu₅Zr has been observed in the past in Cu-Cr-Zr alloys⁴. Based upon the Cu-Zr phase diagram³, the expected phase was Cu₉Zr₂ for a low Zr alloy. It appears that the presence of Cr modifies the activities of Cu and Zr such that the formation of Cu₅Zr is favored over Cu₉Zr₂.

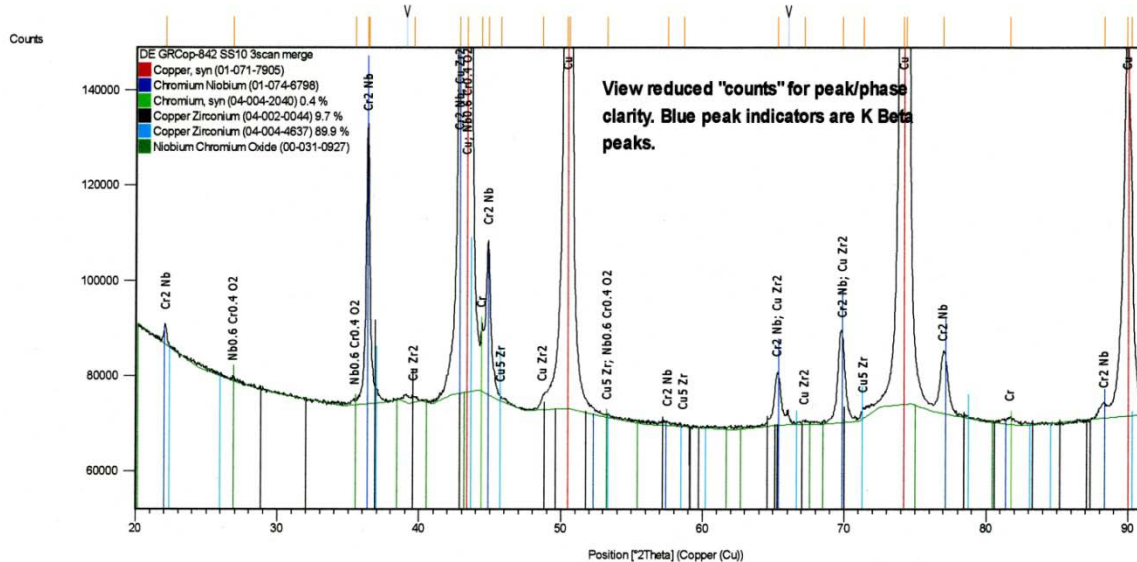


Figure 1 – Detail Of X-Ray Diffraction Scan Results Highlighting Minor Phase Peaks

HEAT TREATMENT DEVELOPMENT

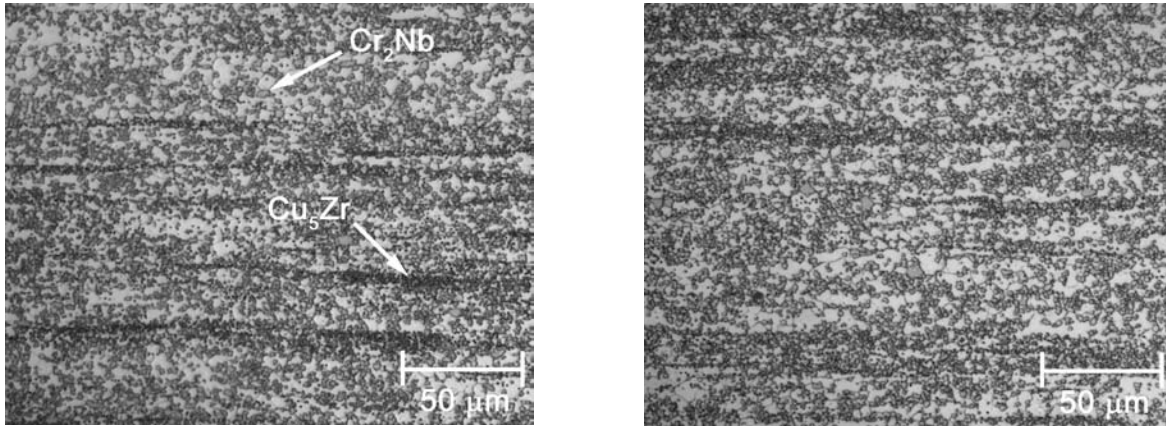
The hardness data for the solution heat treatment development are presented in Table 2. The hardness data from the as-extruded and solution heat treatments (SHT) were analyzed using an Analysis of Variance (ANOVA) test to determine if statistically significant differences at a 95% confidence level existed in the hardnesses measured before and after the heat treatments. Based upon an ANOVA F value of 1.8, it was determined that no statistically significant differences were observed between the four conditions, so optical microscopy and metallurgical principles were used to determine the solution heat treatment temperature. Since the highest temperature would place the highest amount of Zr in solution based upon the phase diagram⁶, 1742 °F (1223 K) was selected.

Table 2 – Extruded GRCop-84Z Hardness Before And After Candidate Solution Heat Treatments

Solution Heat Treatment Temperature	Average Hardness (HR _B)
As-Extruded GRCop-84Z	69.0
1652 °F (1173 K)	67.5
1697 °F (1198 K)	69.5
1742 °F (1223 K)	70.4

Figure 2 shows the as-extruded and 1742 °F (1223 K) solution heat treated sample. Bands of darker material that were identified as Zr-rich using EDS X-ray mapping are seen in both micrographs. The amount of the darker phase decreased with solution heat treatment and was minimized with a 1742

°F (1223 K) solutionizing temperature. Since a higher temperature risked incipient melting, it was decided to use 1742 °F (1223 K) for the solutionizing heat treatment.



(a) As-Extruded

(d) 1742 °F (1223 K)/30 min/WQ

Figure 2 - Optical Micrographs Of GRCo-84Z Samples

Following solutionizing, the samples were aged at 797 °F, 887 °F and 977 °F (698 K, 748 K and 798 K) and air cooled (AC). The hardness of the samples were measured in the solutioned and aged conditions. Table 3 contains the data for the hardness tests. A t-test was used to compare the measured hardnesses to determine if the aging increased the hardness at a 95% confidence level. In all cases, the hardnesses did increase by a statistically significant amount with most samples being 5 to 6 HR_B higher. There were no clearly superior aging temperature or time, so it was decided to use the minimum and maximum values of each for aging the mechanical test specimens.

Table 3 – GRCo-84Z Hardness Before And After Candidate Aging Heat Treatments

Heat Treatment	Condition	Average (HR _B)	Standard Deviation (HR _B)	Increase In Hardness (HR _B)
797 °F/30 min/AC (698 K/30 min/AC)	SHT	69.4	3.2	6.4
	Aged	75.8	2.3	
797 °F/90 min/AC (698 K/90 min/AC)	SHT	72.1	4.4	6.3
	Aged	78.4	2.3	
887 °F/30 min/AC (748 K/30 min/AC)	SHT	73.1	1.3	3.4
	Aged	76.5	2.6	
887 °F/90 min/AC (748 K/90 min/AC)	SHT	72.2	1.4	6.8
	Aged	79.0	2.58	
977 °F/30 min/AC (798 K/30 min/AC)	SHT	73.4	2.3	5.0
	Aged	78.4	3.1	
977 °F/90 min/AC (798 K/90 min/AC)	SHT	72.3	3.5	5.1
	Aged	77.4	3.3	

Tensile Testing

Typical tensile test curves are shown in Figure 3. The stress-strain curves are for samples aged at 977 °F (798 K) for 30 minutes (77 °F (298 K) test) and 90 minutes (932 °F (773 K) test), but the shapes are nearly identical for all GRCo-84Z samples tested. There are two notable features. Unlike most copper alloys, the 77 °F (298 K) curve does not show much decrease in stress after the UTS is achieved, and the total strain is fairly low at about 20%. These samples, when examined after testing, showed mostly uniform strain in the gauge section with minimal necking.

The 932 °F (773 K) stress-strain curve shows that the GRCo-84Z samples yield quickly, achieve UTS shortly thereafter, and then undergoes a great deal of strain prior to failure. Unlike the 77 °F (298 K) test specimens, these specimens showed considerable necking prior to failure.

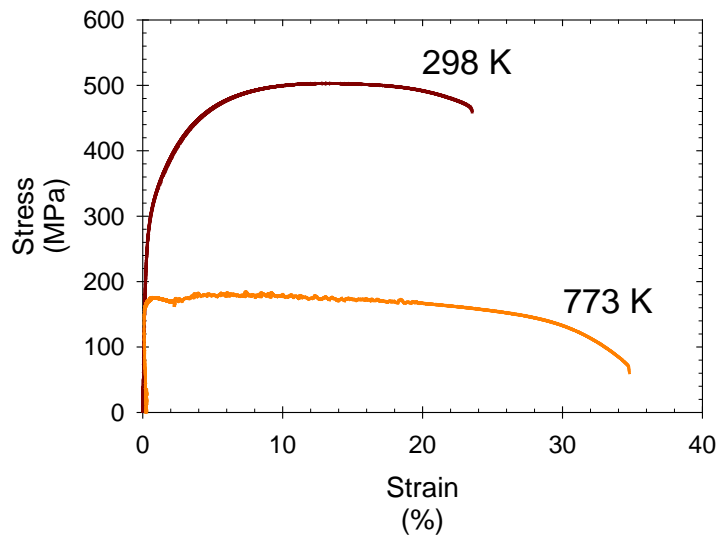


Figure 3 – Typical GRCo-84Z Tensile Test Stress-Strain Curves

The results of the tensile testing are summarized in Figures 4 and 5. The average values for GRCo-84 are also included for comparison. The average room temperature yield strengths of aged specimens were 2% to 21% greater than GRCo-84. The average room temperature UTS increased by 20 to 27% higher for aged GRCo-84Z. Unexpectedly, the average elongation was greatly increased while the reduction in area was decreased at room temperature. This was caused by Zr promoting more uniform elongation in the entire reduced section and less necking at the point of failure. The average elongation increased by 3% to 30% for aged GRCo-84Z. Meanwhile, the average reduction in areas decreased by 24% to 45% for aged GRCo-84Z.

Zr was added primarily to improve the low temperature strength of GRCo-84, but its largest observed effect was upon the 932 °F (773 K) tensile properties. The aged yield strength increased by 36% to 64% while the aged UTS increased by 43% to 68%. The ductility increased at 932 °F (773 K) with the average tensile elongation increasing by 57% to 85%, and the reduction in area increasing by 100% to 128%. At 932 °F (773 K), based upon the stress-strain curves, most of the deformation in the samples occurs after the UTS is achieved but at sufficiently high stresses to still enable plastic deformation in much of the gauge section.

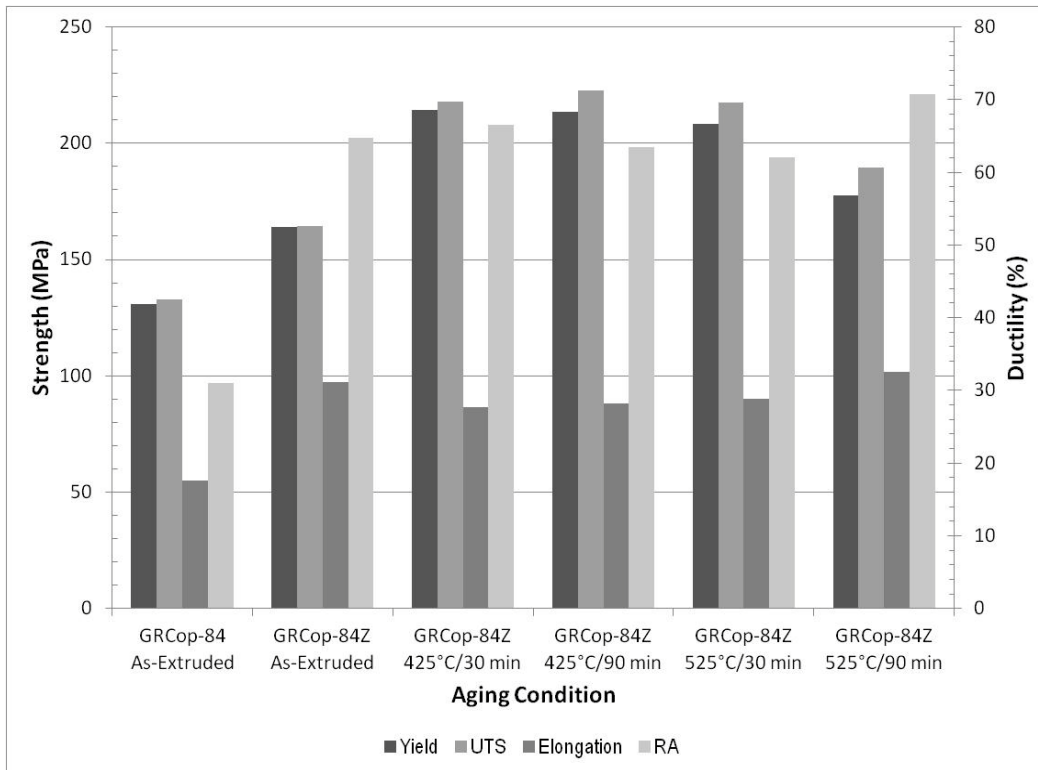


Figure 4 – Room Temperature GRCop-84Z Tensile Test Results

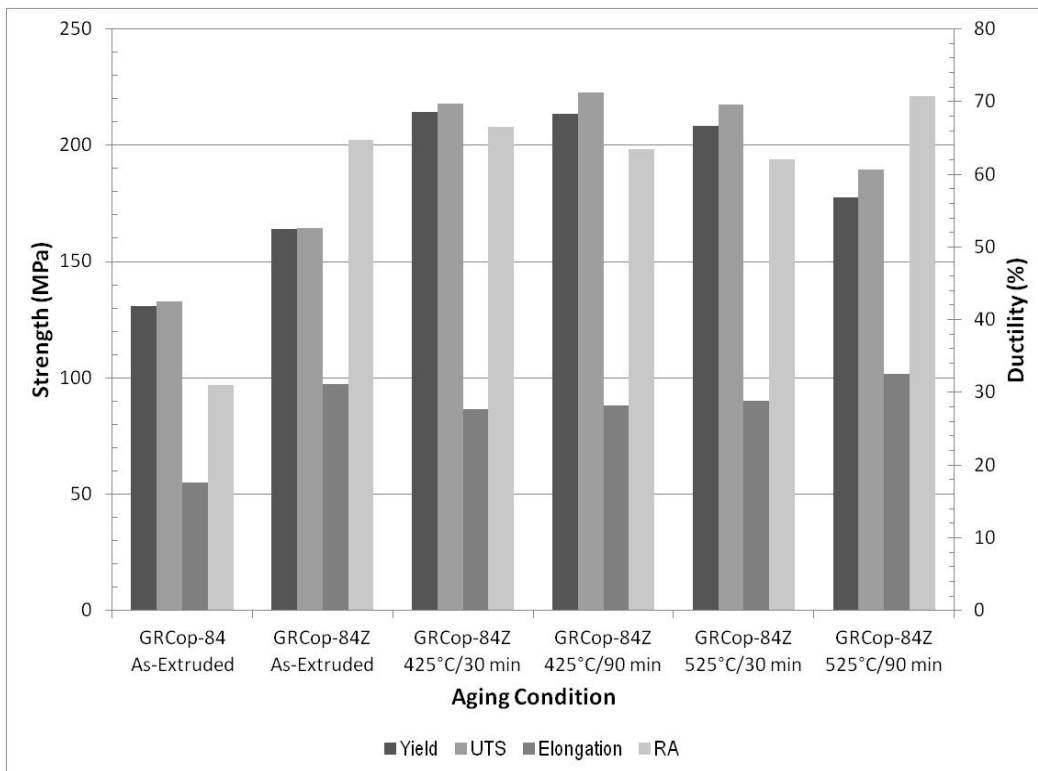


Figure 5 – 932 °F (773 K) GRCop-84Z Tensile Test Results

CREEP TESTING

The results for the 932 °F (773 K) steady-state creep rate are shown in Figures 6, and the results for the 932 °F (773 K) creep life are shown in Figure 7. Data for GRCop-84 are again shown for comparison. During the creep testing of both GRCop-84¹ and GRCop-84Z, primary creep lasted about 10% of the total test time. After primary creep, a gradual transition to second stage or steady-state creep occurred. Steady-state creep lasted for an extended period of time, often nearly half the test. After steady-state creep, there was a very gradual transition to tertiary creep and eventually failure.

Aging the GRCop-84Z clearly has great benefits for creep at 932 °F (773 K). Analysis of the four aged conditions showed that there were no statistically significant differences in the results. This indicates no clear preference for any of the aging heat treatments over this stress range. Since there was no statistical significant differences, the aged GRCop-84Z creep data was pooled, and a single regression performed on the pooled data rather than the individual data sets. Comparing the creep life and creep rate regression curves for the combined aged GRCop-84Z and baseline GRCop-84, the creep rate decreases 38X while the life increases by 19X over the creep stress range tested.

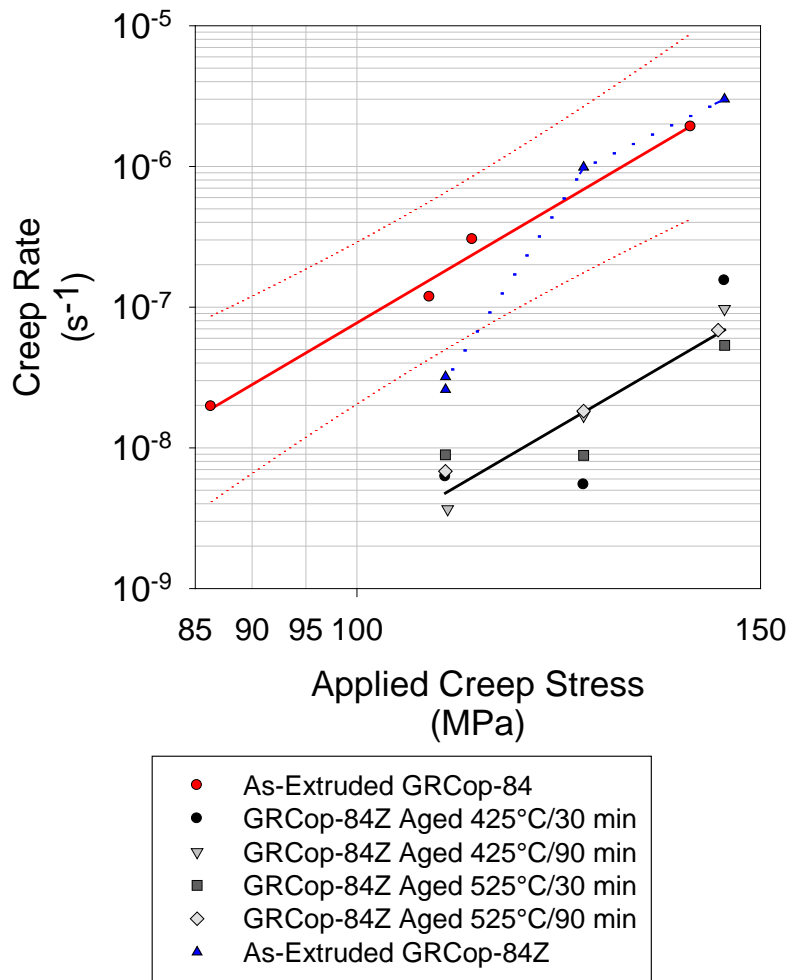


Figure 6 – Creep Rate Of GRCop-84 Z at 773 K

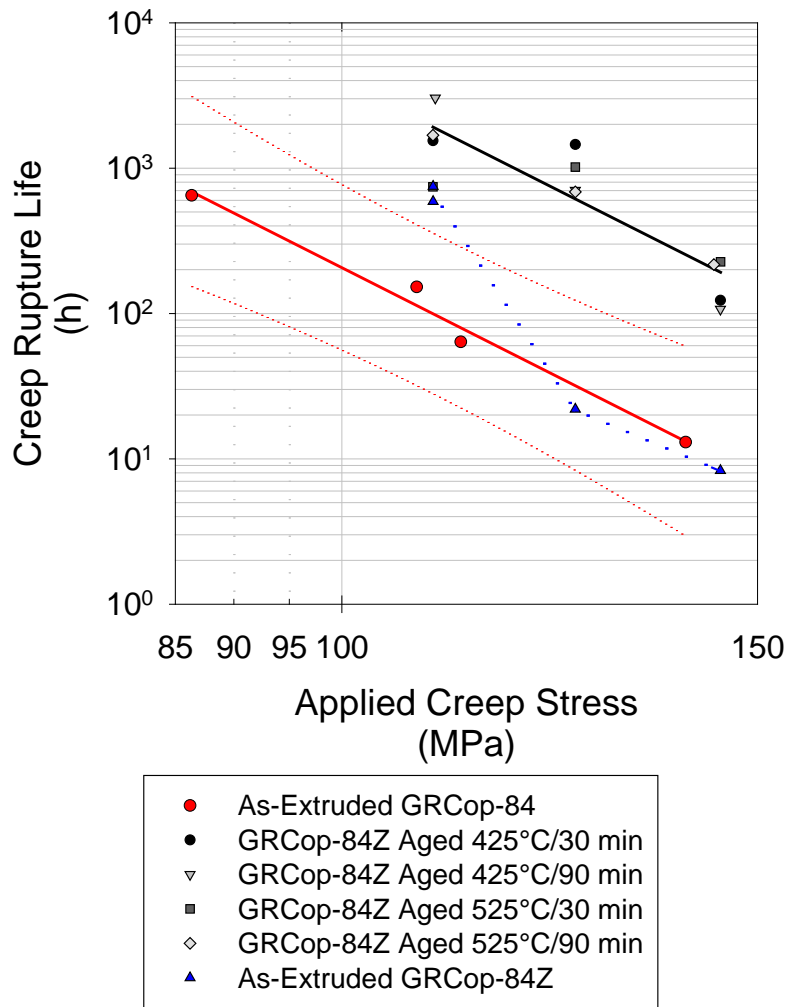


Figure 7 – Creep Life Of GRCo-84Z at 773 K

LOW CYCLE FATIGUE

The room temperature LCF lives of the as-extruded and aged GRCo-84Z samples are shown in Figure 8. The regression line for the life for GRCo-84 and the associated 95% confidence limit is shown in Figure 8 as well for reference. A statistical analysis was conducted, and a small but statistically significant decrease in LCF was found for the GRCo-84Z specimens aged at 797 °F (698 K). The amount was small and, given the small sample size and typically large scatter for LCF lives, was not considered to be of great engineering significance.

The largest difference in LCF behavior was noted when the cyclic strengths at half life were plotted against the plastic strain ranges. As can be seen in Figure 9, all of the aged GRCo-84Z data exceeded the 95% confidence interval for GRCo-84. A statistical analysis confirmed that the aged samples were stronger and also revealed a statistically significant increase for as-extruded GRCo-84Z.

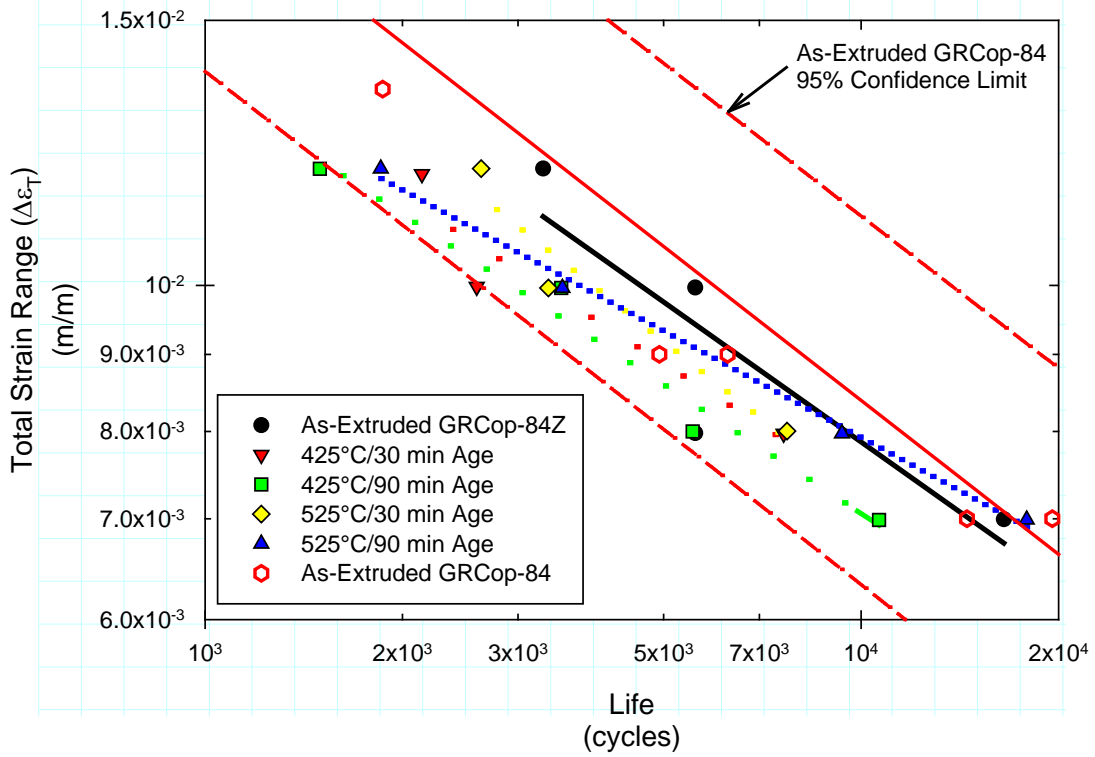


Figure 8 – Fatigue Life At Room Temperature As A Function Of Total Strain Range

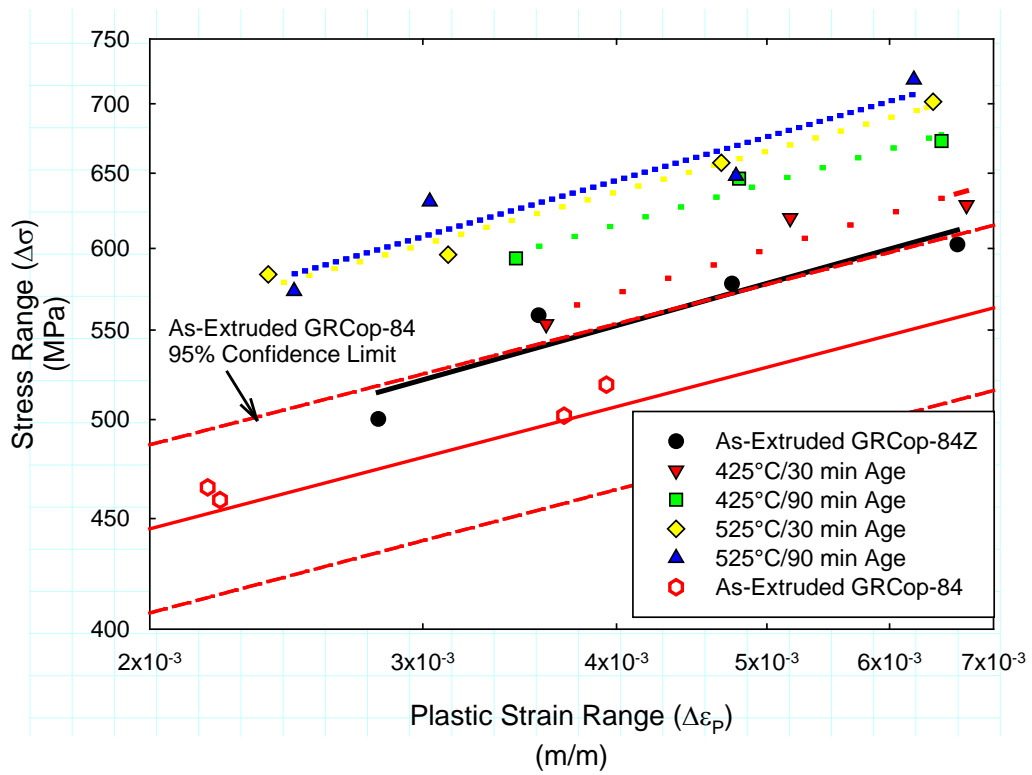


Figure 9 – Cyclic Strength At Room Temperature As A Function Of Plastic Strain Range

DISCUSSION

TENSILE STRENGTH

The tensile test data indicates that the addition of 0.4 wt.% Zr to GRCo-84 had a strongly beneficial effect relative to the baseline as-extruded GRCo-84 properties. It was expected that the benefits would be greatest at room temperature. However, while there were benefits observed at room temperature, the greatest benefits were seen in specimens tested at 932 °F (773 K).

Even the as-extruded GRCo-84Z showed an increase in yield strength. This was likely from a higher total volume fraction of Cr₂Nb and Cu₅Zr precipitates as shown in Figure 2. The Cu₅Zr precipitates can act as impenetrable barriers to dislocation movement and provide additional strengthening. The Cu₅Zr precipitates were expected to contribute approximately 2 vol.% precipitates based upon the alloy composition and the formation of Cu₅Zr precipitates. Beyond adding to the total volume fraction of the precipitates, the Cu₅Zr particles were smaller than the Cr₂Nb particles. As such, they should be more effective at blocking dislocation movement. To estimate the effects of the Cu₅Zr precipitates, the Ashby-Orowan Equation¹² was used. If the simplifying assumptions are made that the precipitates are spherical and widely spaced, the Ashby-Orowan Equation can be expressed as

$$\sigma \cong K \left(\frac{V_f^{1/2}}{r} \right) \ln \left(\frac{r}{b} \right) \quad [1]$$

Here σ is the yield strength of the material (MPa), K is a constant equal to $0.1836 Gb$, G is the shear modulus (MPa), b is the Burgers vector in the slip direction (m), V_f is the volume fraction of precipitate, and r is the average radius of the precipitates (m). While the simplifications may not precisely apply to GRCo-84Z, it is possible to use this equation to estimate order-of-magnitude changes.

Based upon the Ashby-Orowan model, the increase in volume fraction of precipitates from 14% to 16% alone would increase the strength by 7%. Since the Cu₅Zr precipitates are finer, the Ashby-Orowan model also predicts a considerable increase in strength from the reduced precipitate size. No quantitative measurements were made of the Cu₅Zr precipitate size, but, if an estimate of the Cu₅Zr precipitate diameter being one-quarter to one-third the diameter of the Cr₂Nb precipitates is used, and the strengthening of each type of precipitate is assumed to be additive, the total strength increase would be on the order of 23% to 39%. This estimate is consistent with the observed difference in the room temperature yield strengths between GRCo-84 and GRCo-84Z. This indicates that the Cu₅Zr precipitates are acting as expected by supplying an additional strengthening mechanism.

Based upon the 932 °F (773 K) tensile strength and creep properties, the benefits of the Cu₅Zr precipitates persist at 932 °F (773 K) even over fairly long exposure durations. This was somewhat unexpected since it was assumed that they would coarsen to the point of overaging when the specimens were exposed at 932 °F (773 K). The results seem to indicate that overaging is not an issue, and very large increases in strength at elevated temperatures are therefore possible.

CREEP PROPERTIES

The as-extruded GRCo-84Z samples had anomalous results. At the lowest stress (15.8 ksi (109 MPa)), the as-extruded specimens were similar in creep rate and life to the aged GRCo-84Z specimens. At higher stresses (18.1 ksi (125 MPa) and 20.9 ksi (144 MPa)), the creep behavior of as-extruded

GRCop-84Z is near that of GRCop-84. It is unclear why the transition occurs, and time limitations prevented a more detailed examination of the phenomena. It is speculated that the changes may, in part, be due to the activation of a new slip system at the higher stresses. There may also be a transition from diffusional creep to power law creep as the stresses are approaching the 932 °F (773 K) yield stress.

The fine Cu_5Zr precipitates created during aging seem to act as strong barriers to dislocation movement, but it was not possible to perform transmission electron microscopy during the program to determine if this is true. Over the life of the creep test (100 h to 3,000 h for the aged specimens), the Cu_5Zr precipitates do not appear to coarsen to the point where the GRCop-84Z becomes overaged.

The increase in 932 °F (773 K) ductility does not appear to be a major contributing factor to the improvement in creep life. The as-extruded GRCop-84Z specimens have better ductility than the GRCop-84, but only the low stress creep tests demonstrated better lives. If increased uniform elongation was improving creep lives by providing a larger “pool” of ductility and extending the time in steady-state creep, it would be expected that all of the as-extruded GRCop-84Z specimens would exhibit at least some increase in life. This was not observed, and it is unclear at this time why greater improvements were not observed.

The fracture surfaces of the GRCop-84Z creep specimens were examined optically. The failure mechanism appeared to be microvoid coalescence in all cases. This is consistent with GRCop-84 and the GRCop-84Z tensile test specimens. It does not help to explain the differences in the as-extruded GRCop-84Z behavior with stress.

The statistical analysis indicates that the creep rates and lives were offset by a constant amount. This is indicative of the addition of a new, additive strengthening mechanism rather than a fundamental change in strengthening. This is consistent with adding a second strengthening phase that provides Orowan strengthening like the Cr_2Nb precipitates.

LOW CYCLE FATIGUE

It had been hoped that the LCF life of GRCop-84 could be improved by the addition of Zr. As shown in Figure 8, this did not occur. There was no apparent change in life. This was somewhat surprising since, in general, ductility correlates well with the fatigue life of a material as was explained by Coffin and Manson¹³. Materials with large amounts of ductility can absorb and tolerate large amounts of damage prior to failure. The relative room temperature ductility of GRCop-84Z as measured by the tensile elongation is 3.4% to 29.8% greater than GRCop-84, but the ductility as measured by the reduction in area is reduced by 23.9% to 45.2%.

The differing measures of ductility make it unclear if the room temperature LCF lives of GRCop-84Z should increase or decrease. In both cases, the absolute ductility remains above 15%. Hence, the ductility coefficient in the equation for Universal Slopes¹⁴ does not change drastically. Similarly, since the ductility coefficient in the Universal Slopes equation is related directly to the cyclic strain-hardening exponent, and that exponent is identical for GRCop-84 and GRCop-84Z, no change is expected in the slope of the fatigue curve. Taken together, the similarities in the room temperature LCF lives is not unexpected or unusual.

While LCF testing was conducted only at room temperature, some speculation was given to the benefits of Zr on elevated temperature cyclic stresses and LCF lives. As shown in Figure 5, the 932 °F (773 K) tensile strength of aged GRCop-84Z is much greater than GRCop-84. It is anticipated that this

large increase in elevated temperature strength will translate into GRCo-84Z having much greater 932 °F (773 K) cyclic stresses than GRCo-84 and the ability to withstand much higher loads.

Unlike the room temperature tests, the 932 °F (773 K) tensile test data show large increases in both the tensile elongation (57% to 85%) and reduction in area (90% to 128%). Assuming that the elevated temperature LCF lives follow the common trend of increased life with increased ductility and strength as quantified by the Universal Slopes equation, it is believed that the 932 °F (773 K) LCF lives will show benefits from the addition of Zr to GRCo-84. Unfortunately it was not possible to test this hypothesis before concluding the experimental work. It is hoped that additional GRCo-84Z LCF testing at 932 °F (773 K) can be done in the future.

The statistical analyses of the LCF lives and the LCF strengths both indicate that the slopes of the regression lines are statistically equivalent to those for GRCo-84. The addition of Zr therefore acts as an additional strengthening mechanism that does not appear to fundamentally change the LCF behavior. This is consistent with the observations of the other mechanical properties tested.

AGING TIME AND TEMPERATURE

Four combinations of temperature and time were tried to attempt to optimize the mechanical properties of GRCo-84Z. All four were successful in increasing the strength at room temperature and 932 °F (773 K). The 932 °F (773 K) creep properties were also increased dramatically. The LCF lives were not increased, but the LCF stresses at half life were increased. Overall, there was no clearly superior aging heat treatment. Even comparing the aged material to the as-extruded GRCo-84Z did not help to differentiate the four heat treatments tested. This appears to indicate that GRCo-84Z has a very wide range of possible aging times and temperatures. This may prove to be very useful for final aging of manufactured parts where different parts that have undergone different manufacturing processes (cold working, brazing, etc.) may require different heat treatments but similar properties.

SUMMARY AND CONCLUSIONS

The addition of Zr clearly produced improvements in the tensile properties compared to GRCo-84 at both room temperature and 932 °F (773 K). For aged GRCo-84Z at room temperature, the 0.2% offset yield strength was increased between 2% and 21% depending upon the aging treatment. The 932 °F (773 K) yield strength increased even more with gains between 36% and 64%, again depending upon the aging treatment. Similar increases in the UTS and tensile elongations occurred. The reduction in area actually decreased at room temperature as less necking occurred, but it increased 100% to 128% at 932 °F (773 K).

The 932 °F (773 K) creep properties of aged GRCo-84Z showed considerable improvements over GRCo-84. Aged GRCo-84Z samples had a 19X increase in creep life and a 38X decrease in creep rate compared to GRCo-84.

The room temperature LCF lives of GRCo-84Z were generally equal to that of GRCo-84. The stress range at half-life for GRCo-84Z exceeded that of GRCo-84 by 7.2 ksi to 16.7 ksi (50 MPa to 115 MPa) depending upon the heat treatment. Since LCF lives are generally related to ductility as shown in the Universal Slopes equation, it is speculated that the 932 °F (773 K) LCF lives of GRCo-84Z would exceed those of GRCo-84 since it has much greater tensile ductility (>50% increase in elongation and >95% increase in reduction in area). Likewise, the increase in 932 °F (773 K) strength will likely translate into an increased cyclic response stress at 932 °F (773 K).

The addition of Zr to GRCop-84 showed clear benefits in most mechanical properties tested. Solutioning and aging the alloy to produce fine Cu₅Zr precipitates enhanced these benefits. While most of the benefits of Zr were expected to occur at room temperature, in fact the greatest benefits occur at 932 °F (773 K). The increases in properties are generally large and show considerable promise for replacing GRCop-84 with GRCop-84Z to improve rocket engine performance and/or reduce risk in applications where it is possible to solution heat treat and age the part.

FUTURE WORK

Many copper-based alloys containing Zr get additional strengthening from cold work. The Zr appears to retard the annealing process and allow cold work to be retained at 932 °F (773 K) for at least short times¹. It is desired to cold work the GRCop-84Z samples and determine if significant increases in properties occur.

ACKNOWLEDGEMENTS

The authors would like to acknowledge the funding of the work by NASA Glenn Research Center under the Center's Internal Research and Development program.

REFERENCES

1. H.C. de Groh, D.L. Ellis and W.S. Loewenthal, "Comparison of GRCop-84 to Other High Thermal Conductive Cu Alloys," NASA TM-2007-214663, NASA Glenn Research Center, Cleveland, OH, (Feb. 2007).
2. J.J. Esposito and R.F. Zabora, *Thrust Chamber Life Prediction, Vol. 1 – Mechanical and Physical Properties of High Performance Rocket Nozzle Materials*, NASA CR-134806, NASA Lewis Research Center, Cleveland, OH (March 1975).
3. N.J. Grant, A. Lee and M. Lou, *Multiple Hardening Mechanisms For High Strength, High Temperature, High Conductivity Copper Base Alloys*, **High Conductivity Copper and Aluminum Alloys**, E. Ling and P.W. Taubenblat, Eds., The Metallurgical Society of AIME, Warrendale, PA (1984) pp.103-117.
4. F.R. Mollard, E.G. Wickle and A.R. Chaudhry, *Copper-Beryllium For Elevated Temperature Electronic And Electrical Applications*, Ibid, pp. 147-167.
5. J.B. Conway, R.H. Stentz and J. T. Berling, "High Temperature, Low-Cycle Fatigue of Copper-Base Alloys in Argon; Part I - Preliminary Results for 12 Alloys at 1000 °F (538 °C)", NASA CR-121259, NASA Lewis Research Center, Cleveland, OH (Jan. 1973).
6. D. Arias and J.P. Abriata, "Cu-Zr," **Phase Diagrams of Binary Copper Alloys, Monograph Series on Alloy Phase Diagrams, Vol. 10**, P.R. Subramanian, D.J. Chakrabarti and D.E. Laughlin, Eds., ASM International, Materials Park, OH (1994), pp. 497-502.
7. D.L. Ellis, "Observations of a Cast Cu-Cr-Zr Alloy," NASA/TM - 2006-213968, NASA Glenn Research Center, Cleveland, OH (Feb. 2006).
8. P.W. Taubenblat, W.E. Smith and A.R. Graviano, "Properties and Applications of High Strength, High Conductivity Coppers and Copper Alloys," **High Conductivity Copper and Aluminum Alloys**, Eds. E. Ling and P.W. Taubenblat, TMS-AIME, Warrendale, PA, (1984), pp. 19-29.
9. V. Collcut, "High Copper Alloys - High Strength Coppers for Demanding Electrical Applications," Copper Development Association Bulletin, (Sept. 2006). Retrieved from http://www.copper.org/publications/newsletters/innovations/2006/09/high_cu_alloys.html on Nov. 4, 2011.
10. ASTM Standard E-8 - Standard Test Methods For Tension Testing Of Metallic Materials, ASTM International, West Conshohocken, PA.

11. D.L. Ellis and D.J. Keller, "Thermophysical Properties of GRCop-84," NASA CR-210055, NASA Glenn Research Center, Cleveland, OH, (June 2000).
12. M.F. Ashby, Oxide Dispersion Strengthening, AIME Conference Proceedings, New York, NY (1966), p. 143.
13. M.A. Meyers and K.K. Chawla, "21.1.4 Fatigue Strength or Fatigue Life", **Mechanical Metallurgy, Principles and Applications**, Prentice-Hall, Inc., New York, NY (1984), pp. 695-699.
14. S.S. Manson and G.R. Halford, Fatigue and Durability of Structural Materials, ASM International, Materials Park, OH 2006.